

Lecture 2

Interstellar Absorption Lines: Line Radiative Transfer

1. Atomic absorption lines
2. Application of radiative transfer to absorption & emission
3. Line broadening & curve of growth
4. Optical/UV line formation
5. Optical/UV line observations

References: Spitzer Secs. 3.1-3.4
Ay216_06 (JRG)
Dopita & Sutherland Sec. 2.1

1. Optical & UV Absorption Lines

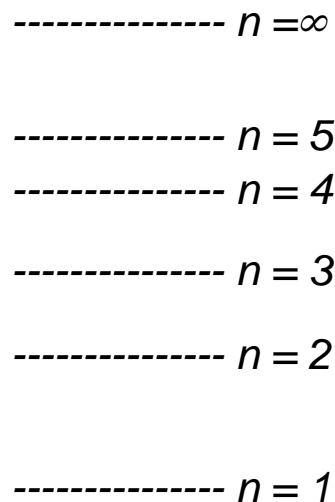
Familiar solar optical doublets, e.g., Fraunhofer Ca II K and Na I D provided early evidence for a pervasive ISM.

These are “resonance” (allowed electric-dipole) transitions, that start from the ground state with an electron going from an *s* to a *p* orbital. Similar transitions occur across the sub- μm band; those below $0.3\ \mu\text{m}$ require space observations. Some important examples are:

H I	[1s]	1216 Å
C IV	[{1s ² } 2s]	1548, 1551 Å
Na I	[{1s ² 2s ² 2p ⁶ } 3s]	5890, 5896 Å
Mg II	[{1s ² 2s ² 2p ⁶ } 3s]	2796, 2803 Å
K I	[{1s ² 2s ² 2p ⁶ 3s ² 3p ⁶ } 4s]	7665, 7645 Å
Ca II	[{1s ² 2s ² 2p ⁶ 3s ² 3p ⁶ } 4s]	3934, 3968 Å

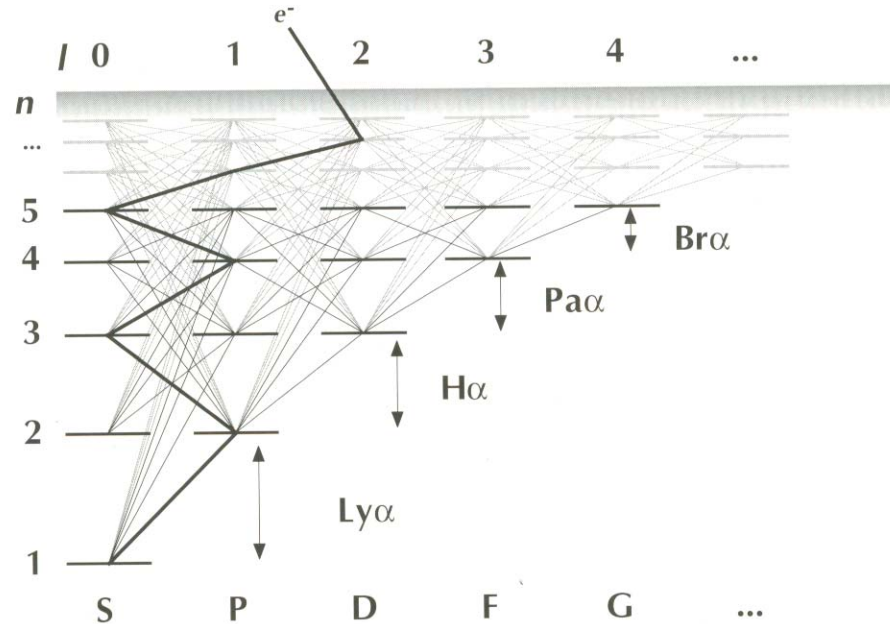
The [{ ... }...] notation gives the electronic configuration, e.g., for MgII, [{1s²2s²2p⁶} 3s] indicates that it is a “one-electron” ion with a 3s electron outside neon-like {1s²2s²2p⁶} closed shell.

Energy Levels of Atomic Hydrogen



Energies depend only on the principle quantum number n :
 $E = -R/n^2$, $R = 13.6$ eV,

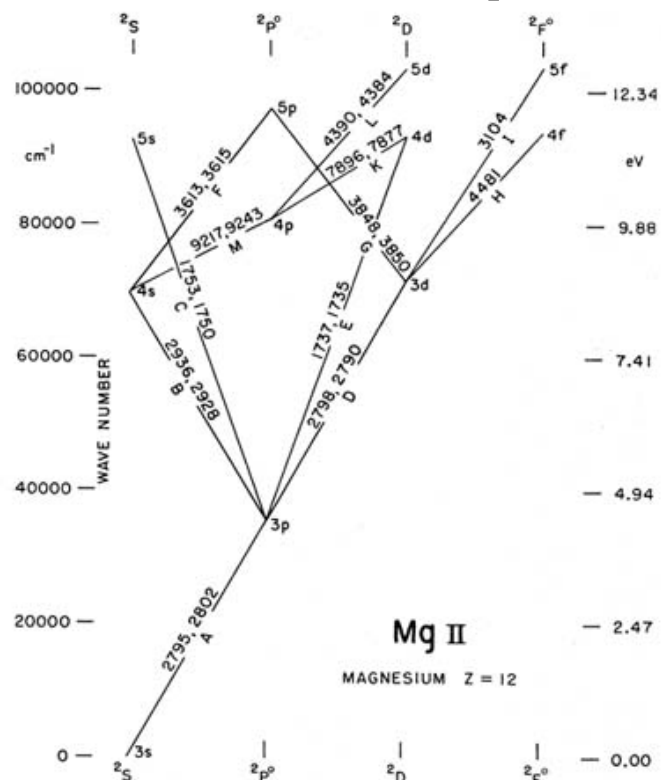
The levels are $2n^2$ -fold degenerate. The orbital quantum number l ranges from $l = 0$ to $n-1$ & the spin quantum number $s = 1/2$



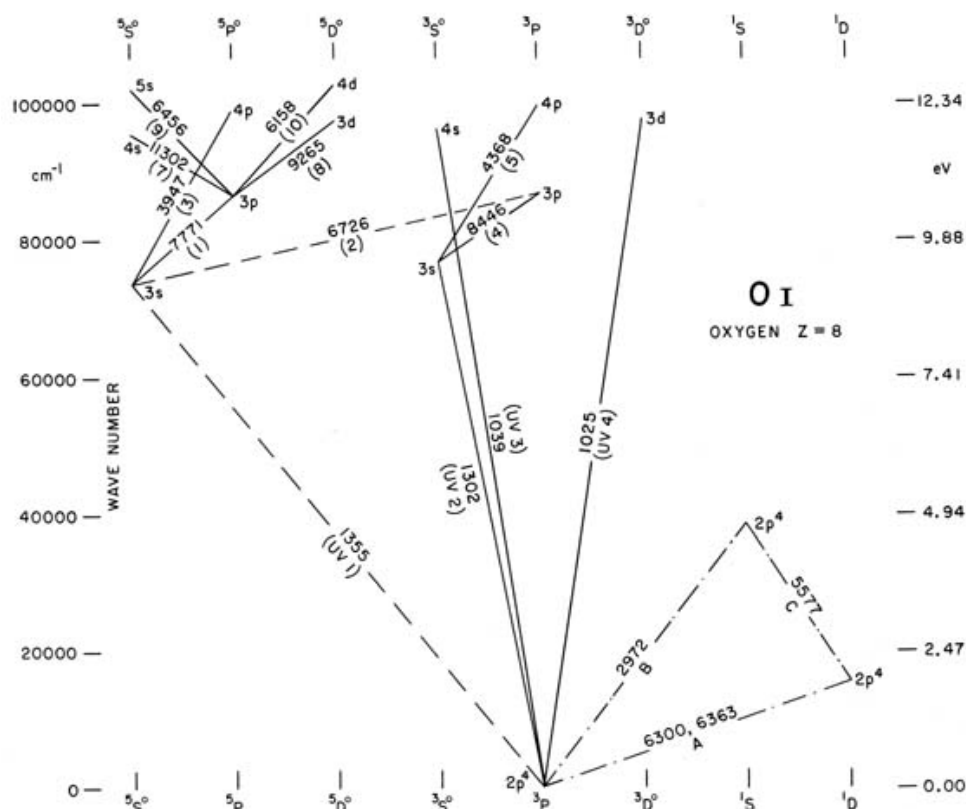
The degenerate levels are spread out according to orbital angular momentum (at top), in a format known as a **Grotrian Diagram**.

The solid line indicates the main transitions that follow from a particular recombination event.

Sample Grotrian Diagrams



Mg II [$\{1s^22s^22p^6\}3s\]$ (2S)



O I [$1s^22s^22p^4$] (3P)

Spectroscopic notation for multi-electron atoms: $2S+1L_J$;
 S , L , & J ($J = L + S$) are total spin, total orbital, and total
 angular momentum quantum numbers, all conserved for
 motion in a central potential.

Observations of Absorption Lines

HST GHRS

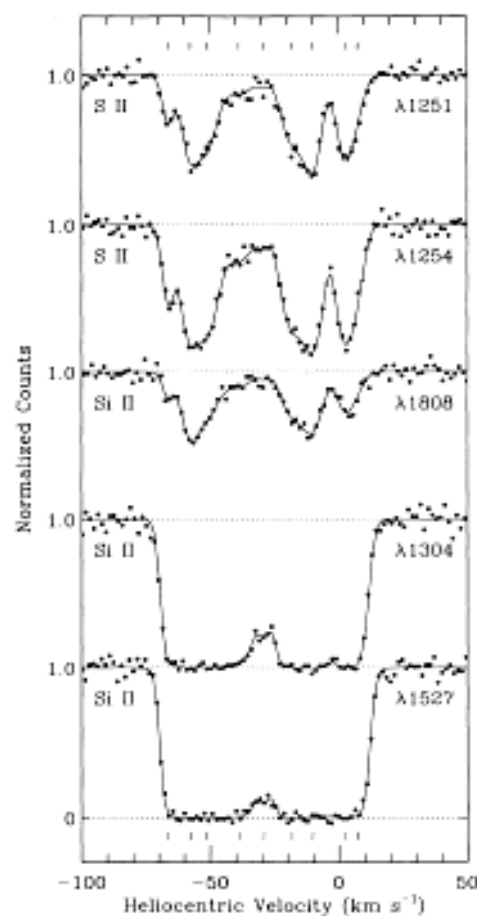


FIG. 2a

At resolution, $R = > 10^4$ (30 km/s), absorption lines break up into Doppler shifted components.

Interstellar lines through the halo towards HD 93521 reveal velocities spanning ~ 90 km/s.

FUSE operates below 1100 Å and can detect H & D Ly- α lines, as discussed in Problem 1.

FUSE

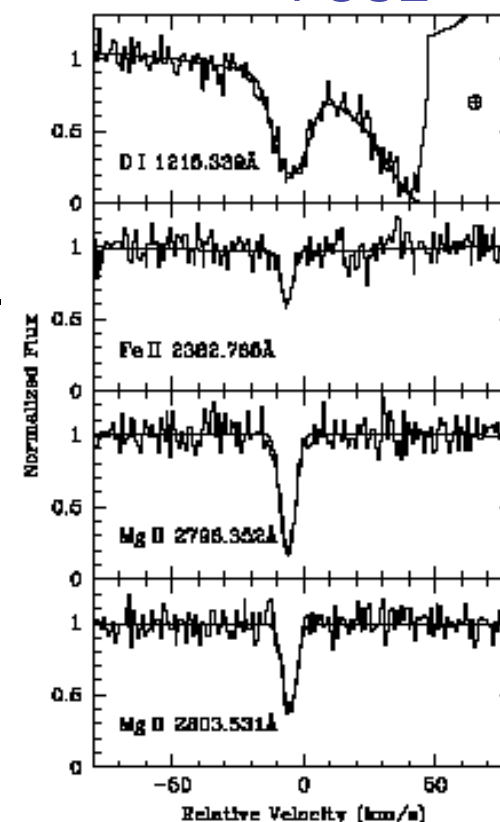


FIG. 1.—Absorption profiles of D I, Fe II, and Mg II are plotted as a function of heliocentric velocity. The histograms are the FUSE echelle measurements, and the smooth line is the single-component fit. No evidence for a second velocity component is seen. The D I line sits on the broad wing of the interstellar H I Ly α profile; the truncated peak at 65 km s⁻¹ in the D I profile is geocoronal Ly α emission.

Halo star HD 93521
Spitzer & Fitzpatrick (1993)

White Dwarf Hz 43A
Krut et al. (2002)

2. Application of Radiative Transfer to Emission and Absorption

We assume some knowledge of radiative transfer, which is founded on the *specific intensity* I_ν , defined as the energy passing through a unit area at an θ angle in unit time, area, solid angle and frequency:

$$dE_\nu = I_\nu dA \cos \vartheta d\Omega d\nu dt$$

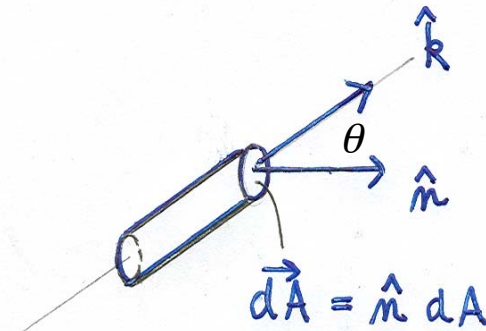
Standard treatments of radiative transfer are widely available:

Rybicki & Lightman Ch.1

Spitzer Ch. 3

Shu I Chs. 1-4

McKee AY216_06, Lec. 2



The Equation of Transfer

The intensity satisfies the equation of transfer

$$\frac{dI_\nu}{ds} = -\kappa_\nu I_\nu + j_\nu$$

Shu shows that I_ν may be considered a Boltzmann-like distribution function for photons, The equation of transfer corresponds to the Boltzmann transport equation; the source term is the emissivity j_ν and the absorption rate $-\kappa_\nu I_\nu$ is the loss term. We next define the optical depth τ_ν through the differential absorption in a distance ds and also define the “source function” S_ν ,

$$d\tau_\nu = \kappa_\nu ds \qquad S_\nu \equiv j_\nu / \kappa_\nu$$

The equation of transfer now assumes the form,

$$\frac{dI_\nu}{d\tau_\nu} = -I_\nu + S_\nu$$

and its solution for a slab is:

$$I_\nu(\tau_\nu) = I_\nu(0) e^{-\tau_\nu} + \int_0^{\tau_\nu} S_\nu(\tau'_\nu) e^{-(\tau_\nu - \tau'_\nu)} d\tau'_\nu$$

The Emission Coefficient

The emissivity j_ν is the rate at which energy is emitted per unit volume, solid angle, frequency and time. For line emission from an upper level k to lower level j , we integrate over frequency to get the line emission coefficient,

$$j_{jk} = \int_{line} j_\nu d\nu$$

This is usually expressed in terms of the Einstein A_{kj}

$$4\pi j_{jk} = n_k h\nu_{kj} A_{kj}$$

The factor 4π arises from integrating over all angles. The units are $\text{erg cm}^{-3} \text{s}^{-1}$, since the units of A_k over s^{-1}

The Absorption Coefficient

The absorption coefficient for radiative excitation from a *lower* level j to an *upper* level k is determined by the *atomic absorption cross-section* (units cm^2) defined by $\kappa_\nu = n_j s_\nu$. The frequency integrated absorption coefficient is

$$\kappa_{jk} = \int_{line} \kappa_\nu d\nu = n_j \int_{line} s_\nu d\nu \equiv n_j s_{jk}$$

It is related to the Einstein B-coefficients:

$$\kappa_{jk} = \frac{h\nu_{jk}}{c} \left(n_j B_{jk} - n_k B_{kj} \right)$$

gives absorption rate \uparrow
from level j up to level k

\uparrow gives the rate of
stimulated emission from
level k down to level j

Note that the integrated quantity s_{jk} has the units of $\text{cm}^2 \text{s}^{-1}$, and that it can be related to the B -coefficients, as will be done in slide 11.

Review of the Einstein *A* & *B* Coefficients

The Einstein *A*-coefficient gives the rate of spontaneous decay.
The relations between the *A* and *B* coefficients,

$$g_j B_{jk} = g_k B_{kj} \qquad B_{kj} = \frac{c^3}{8\pi h \nu_{jk}^3} A_{kj}$$

can be derived from the equation of radiative balance for levels *k* and *j* for a radiation field with spectral energy distribution u_ν

$$u_\nu (n_j B_{jk} - n_k B_{kj}) = n_k A_{kj}$$

by assuming complete thermodynamic equilibrium for both the levels *j* and *k* and the radiation field. They can also be related to emission and absorption *oscillator strengths*, which are essentially QM matrix elements,

$$A_{kj} = \frac{8\pi^2 e^2 \nu^2}{m_e c^3} f_{kj} \qquad g_k f_{kj} = g_j f_{jk}$$

The Integrated Cross Section

With these facts on the B -coefficients, the integrated cross section is:

$$s_{jk} = \int_{line} s_{\nu} d\nu = \int_{line} \frac{\kappa_{\nu}}{n_j} d\nu = \frac{h\nu_{jk}}{c} \left(B_{jk} - \frac{n_k B_{kj}}{n_j} \right) = \frac{h\nu_{jk}}{c} B_{jk} \left(1 - \frac{n_k g_i}{n_j g_k} \right)$$

Thermal equilibrium (TE) level populations are now labeled by an asterix,

$$\frac{n_k^*}{n_j^*} = \frac{g_k}{g_j} e^{-h\nu_{jk}/kT}$$

and *departure coefficients* b_j relate the true level populations (n) to thermal equilibrium populations (n^*), as in $b_j = n_j / n_j^*$. Then s_{jk} is

$$s_{jk} = s_u \left(1 - \frac{n_k g_i}{n_j g_k} \right) = s_u \left(1 - \frac{b_k}{b_j} e^{-h\nu/kT} \right)$$

where

$$s_u \equiv (h\nu_{jk}/c) B_{jk} = (\pi e^2 / m_e c) f_{jk}$$

is the integrated absorption cross-section *without* stimulated emission.

Integrated Cross Section: Limiting Cases

$h\nu \gg kT$ -- Stimulated emission is unimportant; pure absorption dominates

$$s_{jk} = s_u \left(1 - \frac{b_k}{b_j} e^{-h\nu/kT} \right) \approx s_u$$

$h\nu \ll kT$ -- Stimulated emission is important. Expand the exponential and introduce the oscillator strengths to find

$$s_{jk} \approx s_u \left[1 - \frac{b_k}{b_j} (1 - h\nu/kT) \right] = \frac{\pi e^2}{m_e c} f_{jk} \frac{h\nu}{kT} \left[\frac{b_k}{b_j} - \frac{kT}{h\nu} \left(\frac{b_k}{b_j} - 1 \right) \right]$$

If the levels are in TE,

$$s_{jk} \approx \frac{\pi e^2}{m_e c} f_{jk} \frac{h\nu}{kT}$$

For HI 21 cm at 80 K, the correction is huge: $h\nu/kT \approx 8 \times 10^{-4}$.

NB Masers are an example of extreme non-LTE. The absorption term is emissive because the level populations are inverted ($n_k > n_j$).

3. Line Shape & Broadening

Rewrite the absorption cross section as $s_\nu = s \phi(\nu)$ (dropping the line index jk) and introduce the *line shape function* $\phi(\nu)$ with unit normalization,

$$\int_{line} \phi(\nu) d\nu = 1$$

Assume that the absorber is in a system moving with a *line of sight velocity* w , and introduce the notation:

ν_0 = rest frequency

$\nu'_0 = \nu_0 (1 - w/c)$ = Doppler shifted frequency

$\Delta\nu = \nu - \nu_0$

The absorption profile ϕ_1 for an atom depends on $\nu - \nu'_0$,

$$\begin{aligned}\phi_1 &= \phi_1(\nu - \nu'_0) \\ &= \phi_1(\nu - \nu_0 [1 - w/c]) \\ &= \phi_1(\Delta\nu + \nu_0 w/c)\end{aligned}$$

1. Natural Line Broadening

Start with the *general* formula for the line-shape function or a collection of atoms

$$\phi(\nu) = \int_{-\infty}^{\infty} P(w) \phi_1(\Delta\nu + \nu_0 w / c) dw$$

where $P(w)$ is the velocity distribution of the gas

Natural line broadening is due to the finite lifetimes of the upper and lower states (Heisenberg Uncertainty Principle), i.e., atoms absorb and emit over a range of frequencies near ν_0 , and generate a “Lorentzian” line shape

$$\phi_1(\nu) = \frac{1}{\pi} \frac{\gamma_k}{\gamma_k^2 + \Delta\nu^2}$$

The width for an atom at rest ($w = 0$) is

$$\gamma_k = \frac{1}{4\pi} \sum_{k>i} A_{ki}$$

Natural Line Broadening (cont'd)

Natural line widths are very small, e.g., for the electric-dipole H I Ly α transition,

$$A_{21} = 6 \times 10^8 \text{ s}^{-1}, \quad \nu = 2 \times 10^{15} \text{ Hz}, \quad \gamma_k / \nu = 3 \times 10^{-8}$$

For comparison with measured line widths, typically of order km/s, this corresponds to a velocity width,

$$\Delta w = (\gamma_k / \nu) c = 9 \text{ m/s}$$

Forbidden lines are even narrower.

Other broadening mechanisms are caused by:

Stark & Zeeman effects

Collisions (“pressure broadening”)

At low ISM densities, “pressure broadening” is only relevant for radio recombination lines.

Case 2. Doppler Broadening

The velocity distribution is Gaussian

$$P(w) = \frac{1}{\sqrt{\pi} b} e^{-(w/b)^2}$$

For a Maxwellian at temperature T

$$b^2 = \frac{2kT}{m} + 2\sigma_{turb}^2$$

where m is the mean molecular mass and σ_{turb} is the dispersion of the turbulent velocities.

The total dispersion is related to the Gaussian parameter by $\sigma = b/2^{1/2}$.

$$b_{th} \approx 0.129 (T/A)^{1/2} \text{ km s}^{-1} \quad (A = \text{atomic mass})$$

$$FWHM = 2 \sqrt{(2 \ln 2)} \sigma \approx 2.355 \sigma.$$

Case 3. Voigt Profile

Convolving Doppler and natural broadening,

$$\phi(\nu) = \int_{-\infty}^{\infty} P(w) \phi_1(\Delta\nu + \nu_0 w / c) dw$$

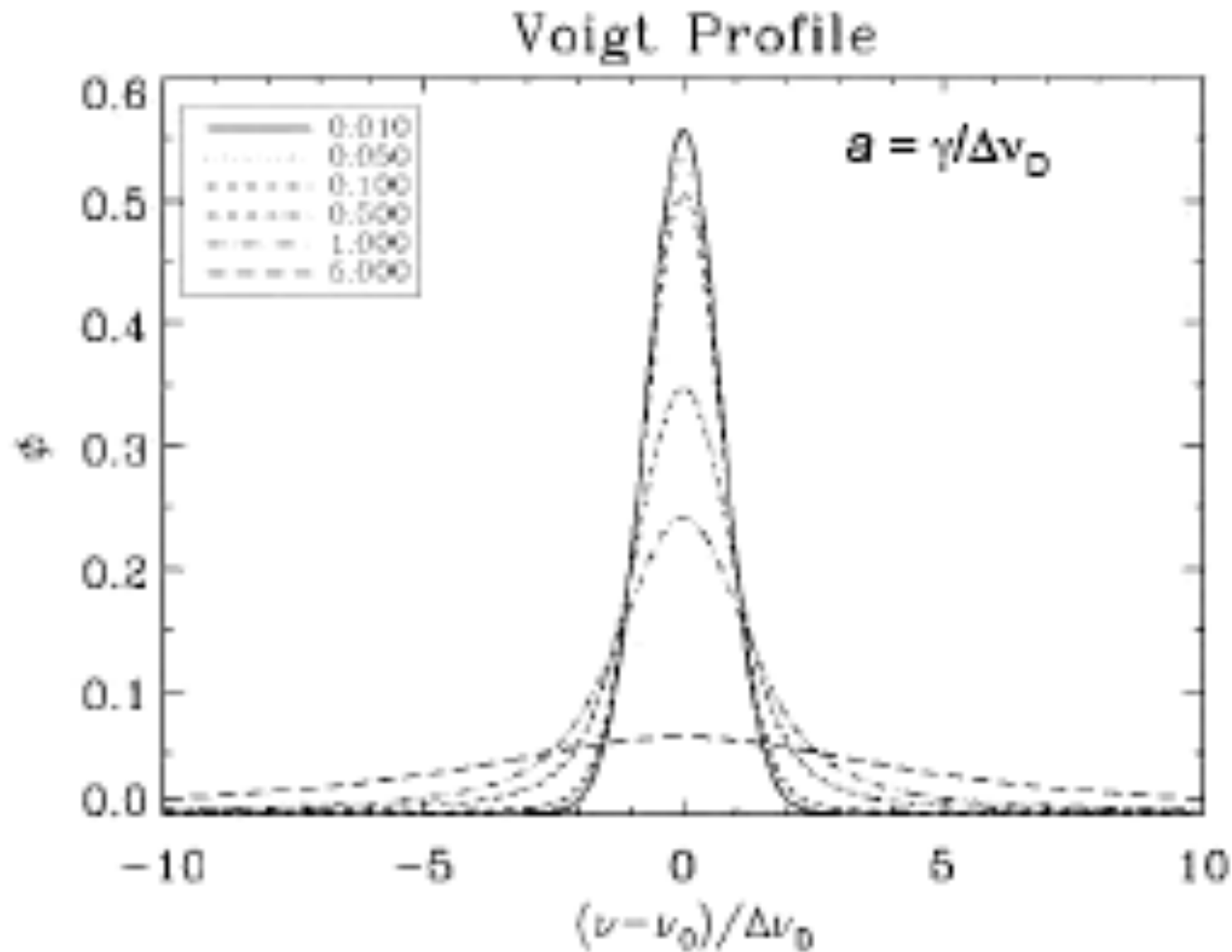
yields the **Voigt profile**

$$\phi(\nu) = \frac{1}{\sqrt{\pi} b} \int_{-\infty}^{\infty} e^{-(w/b)^2} \frac{1}{\pi} \frac{\gamma_k}{\gamma_k^2 + (\Delta\nu + \nu_0 w / c)^2} dw$$

Define the Doppler width, $\Delta\nu_D = (\nu_0 / c) b = b / \lambda_0$, to get

$$\phi(\nu) = \frac{1}{\pi^{3/2} b} \int_{-\infty}^{\infty} e^{-(w/b)^2} \frac{\gamma_k}{\gamma_k^2 + (\Delta\nu + \Delta\nu_D w / b)^2} dw$$

The Voigt profile (evaluated numerically) depends on the ratio of the natural to the Doppler widths



Limiting Forms of the Voigt Profile

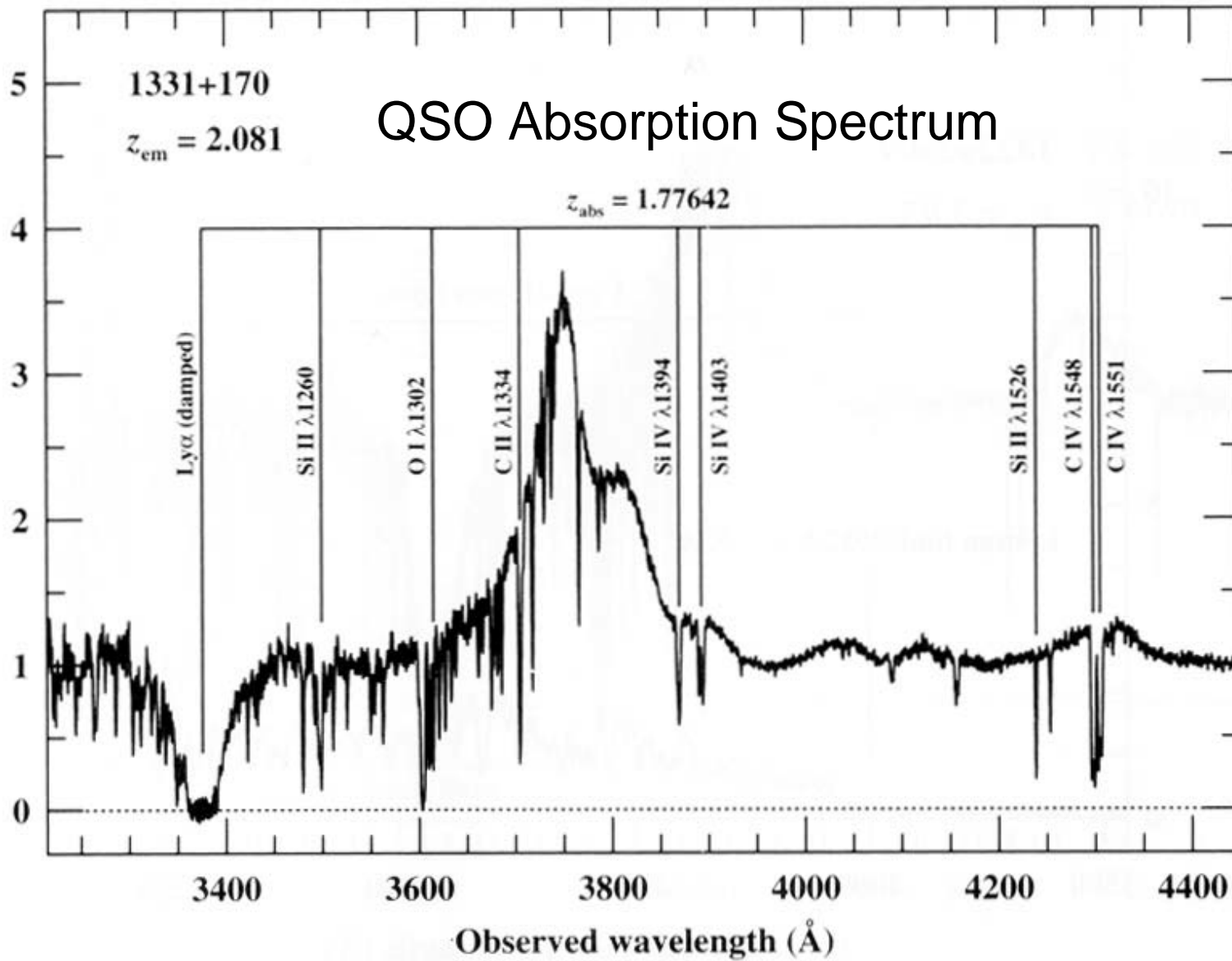
1. Approximating the natural line function by a delta-function recovers the Doppler profile.

$$\phi(\nu) = \frac{1}{\sqrt{\pi} \Delta \nu_D} e^{-(\Delta \nu / \Delta \nu_D)^2}$$

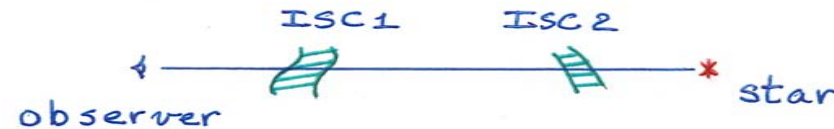
2. For large ($\Delta \nu \gg \Delta \nu_D$) the slowly-decreasing damping wings dominate (and come out of the general convolution integral) to yield the characteristic Lorentzian profile wings:

$$\phi(\nu) = \frac{\gamma_k}{\pi \Delta \nu^2}$$

Doppler Cores and Damping Wings

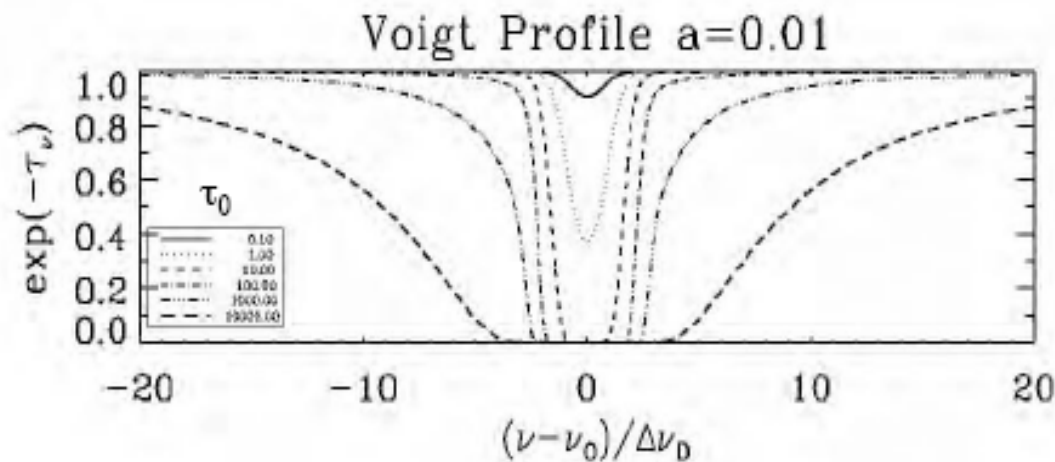


4. UV/Visible Absorption Line Formation



Neglect stimulated emission ($h\nu \gg kT$), assume pure absorption and a uniform slab. The equation of radiative transfer without the emissivity term has the solution,

$$I_\nu = I_\nu(0)e^{-\tau_\nu}, \quad \tau_\nu = N_l s_\nu$$



Ideally, measuring the frequency-dependent line profile determines τ_ν . Finite spectral resolution, signal to noise (S/N), etc., often make an *integrated observable* called **equivalent width** more useful.

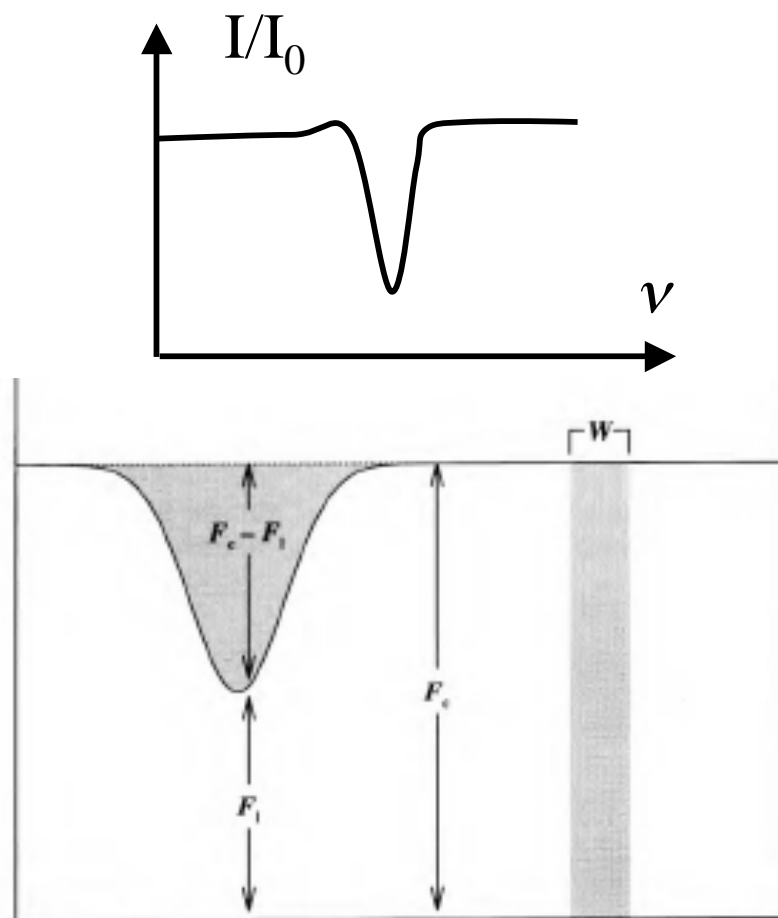
Equivalent Width

$$W_\nu \equiv \int_{-\infty}^{\infty} \frac{I_\nu(0) - I_\nu}{I_\nu(0)} d\nu = \int_{-\infty}^{\infty} (1 - e^{-\tau_\nu}) d\nu$$

W_ν is the width of the equivalent rectangular profile from 0 to $I(0)$ with the same area as the actual line. The units are Hz.

More common is the quantity in terms of wavelength W_λ , measured in Å or mÅ, related as:

$$W_\lambda / \lambda = W_\nu / \nu$$



Curve of Growth: Linear Regime

Optically thin limit: $\tau_0 \ll 1$

$$W_\nu = \int_{-\infty}^{\infty} \tau_\nu d\nu = N_j \int_{-\infty}^{\infty} \sigma(\nu) d\nu = N_j \frac{\pi e^2}{m_e c} f_{lu}$$

τ_0 is the optical depth at line center,

$$\tau_0 = \frac{\lambda_0}{\sqrt{\pi} b} N_j s = N_j \frac{\sqrt{\pi} e^2}{\Delta \nu_D m_e c} f_{jk}$$

Since $W_\nu \propto N_j$, this is known as the linear regime for the curve of growth:

$$\frac{W_\lambda}{\lambda} = 0.885 N_{j,17} f \lambda_{-5}$$

Units: for column density, $10^{17} N_{17} \text{ cm}^{-2}$, for wavelength, $1000 \lambda_{-5} \text{ \AA}$

Nonlinear Portion of the Curve of Growth

For moderately large, i.e., not too large optical depths Doppler broadening suffices and its limit for large optical depths is

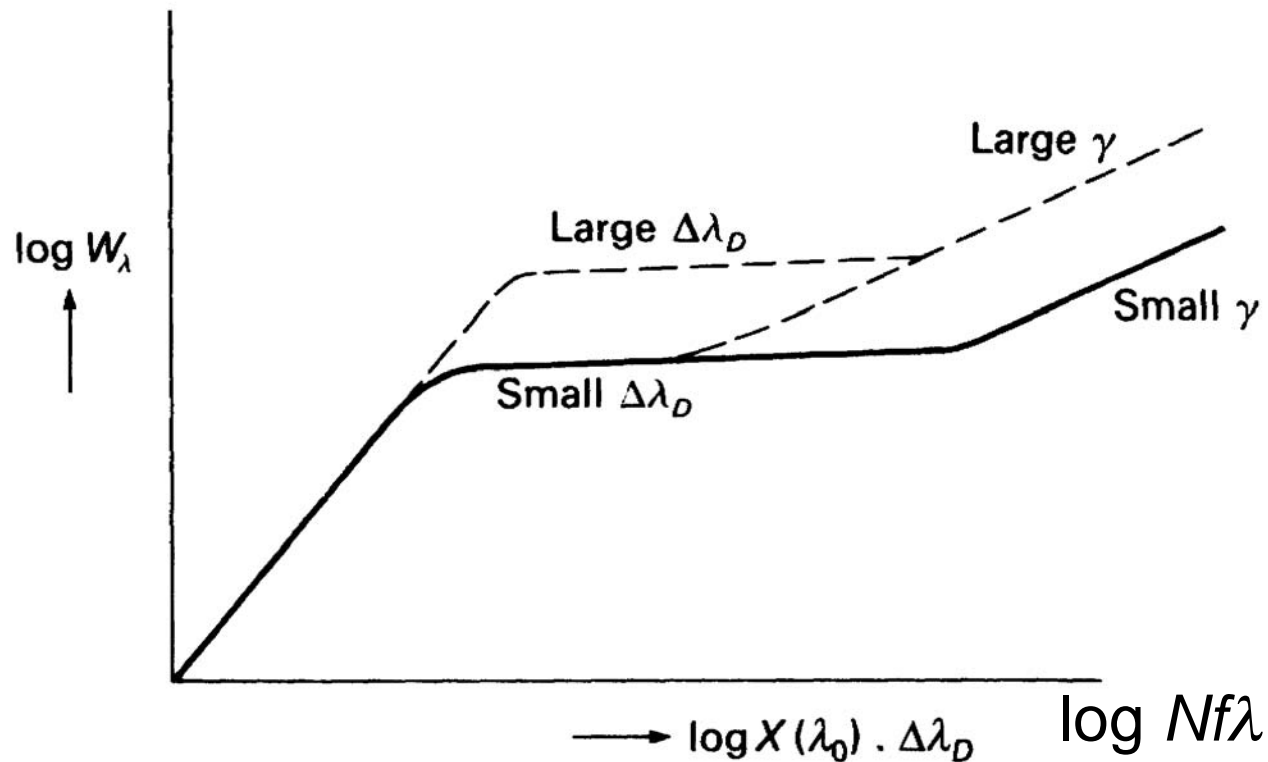
$$W_{\lambda} \approx \int_{-\infty}^{\infty} \left\{ 1 - \exp \left[-\frac{N_j s}{\sqrt{\pi} \Delta \nu_D} e^{-(\Delta \nu / \Delta \nu_D)^2} \right] \right\} d\lambda \xrightarrow{\tau_0 \rightarrow \infty} \frac{2b\lambda}{c} \sqrt{\ln(\tau_0)}$$

For large τ_0 , the light from the source near line center is absorbed, i.e., the absorption is “saturated”. Far from line center there is partial absorption, and W_{λ} grows slowly with N_j ; this is the *flat portion* of the curve of growth.

For very large τ_0 , the Lorentzian wings take over, and generate the *square-root portion* of the curve of growth

$$W_l / \lambda = (2/c) (\lambda 2N_j s \gamma_k)^{1/2}$$

Schematic Curve of Growth



The departure from linear depends on the Doppler parameter; broader Doppler lines remain longer on the linear part of the curve of growth.

NB The origin of this figure has been lost. The abscissa label is $\log Nf\lambda$.

Summary of Curve of Growth Analysis

The goal is to determine column density N_j from the measured equivalent width, which increases monotonically but non-linearly with column N_j .

There are three regimes, depending on optical depth at line center:

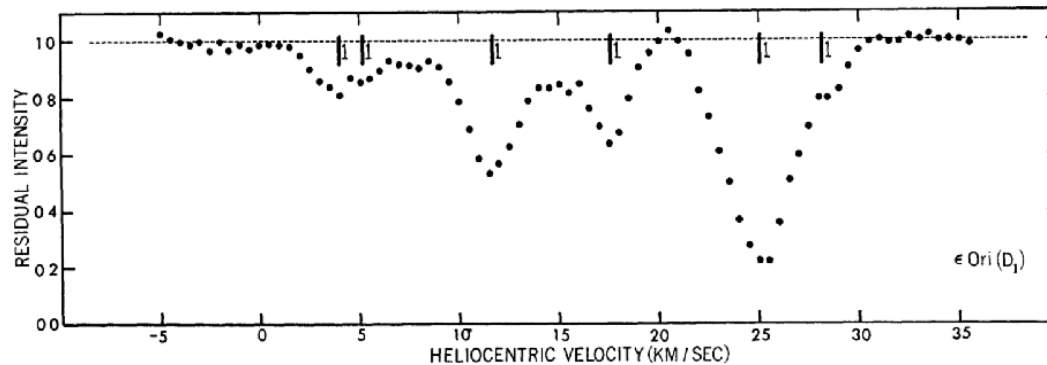
$\tau_0 \ll 1$, linear

$\tau_0 > 1$, large flat

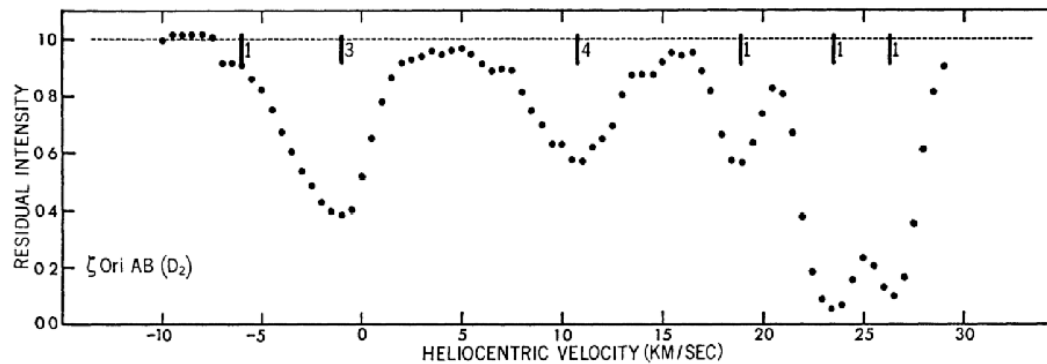
$\tau_0 \gg 1$, square-root (“damping”)

Unfortunately, many observed lines fall on the insensitive *flat* portion of the curve of growth.

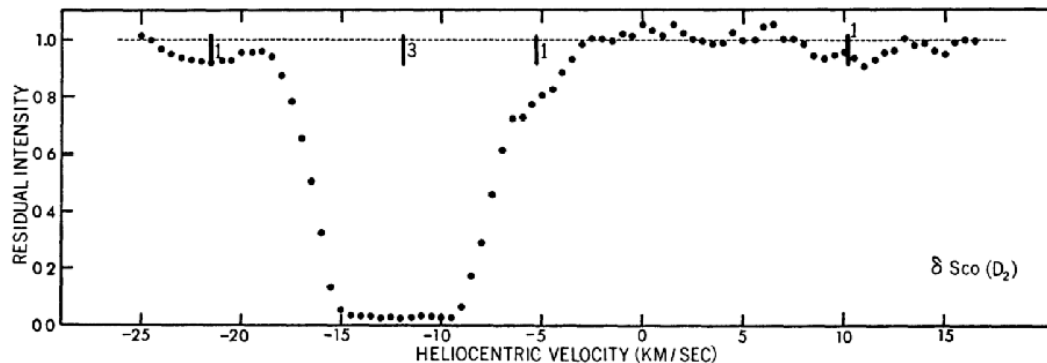
Illustrating the Three Parts of the Curve of Growth for Interstellar Na I Absorption Lines



Linear - flat



Flat



Square-root

5. Optical/UV Absorption Line Observations

Require bright background sources with little obscuration by dust:

$$d < 1 \text{ kpc}, \quad A_V < 1 \text{ mag} \quad \text{or} \quad N_H < 5 \times 10^{20} \text{ cm}^{-2}$$

Strong Na I lines are observed in every direction:

- same clouds are seen in H I emission and absorption,
- also seen in IRAS 100 μm cirrus \Rightarrow CNM

But the H column densities (and abundances) require UV observations of $\text{Ly}\alpha$.

Absorption Lines for an Extragalactic Source

Absorption line spectra of an interstellar cloud seen towards a quasar.

Note the mm absorption lines of HCO⁺ at the bottom.

Molecular lines are common at radio
As well as optical and UV wavelengths.

Figure from Snow & McCall,
ARAA 44 367 2006

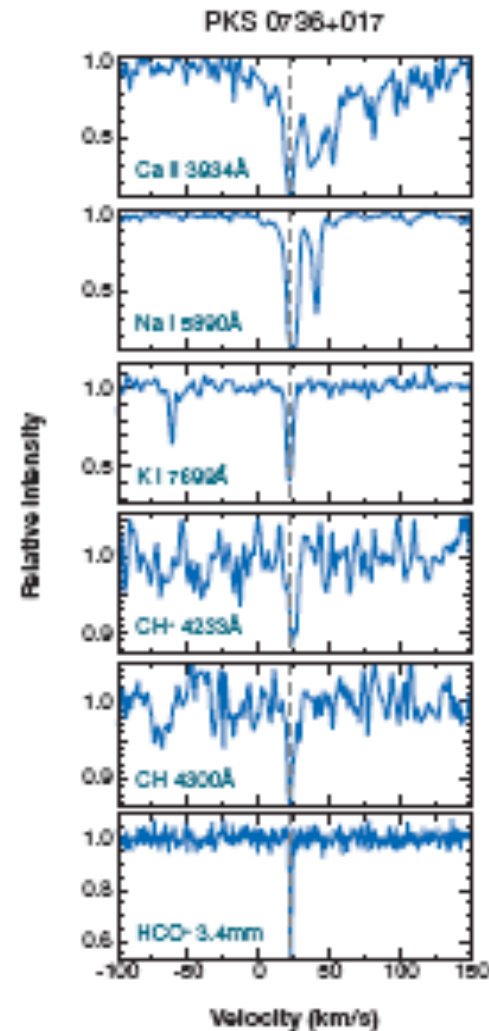


Figure 3

Comparison of optical and millimeter-wave spectra of PKS 0736 + 017, adapted from Tippe (2004). The HCO⁺ data are from Lucas & Liszt (1996).

UV Absorption Lines towards ς Oph

(probably the best studied diffuse interstellar cloud)

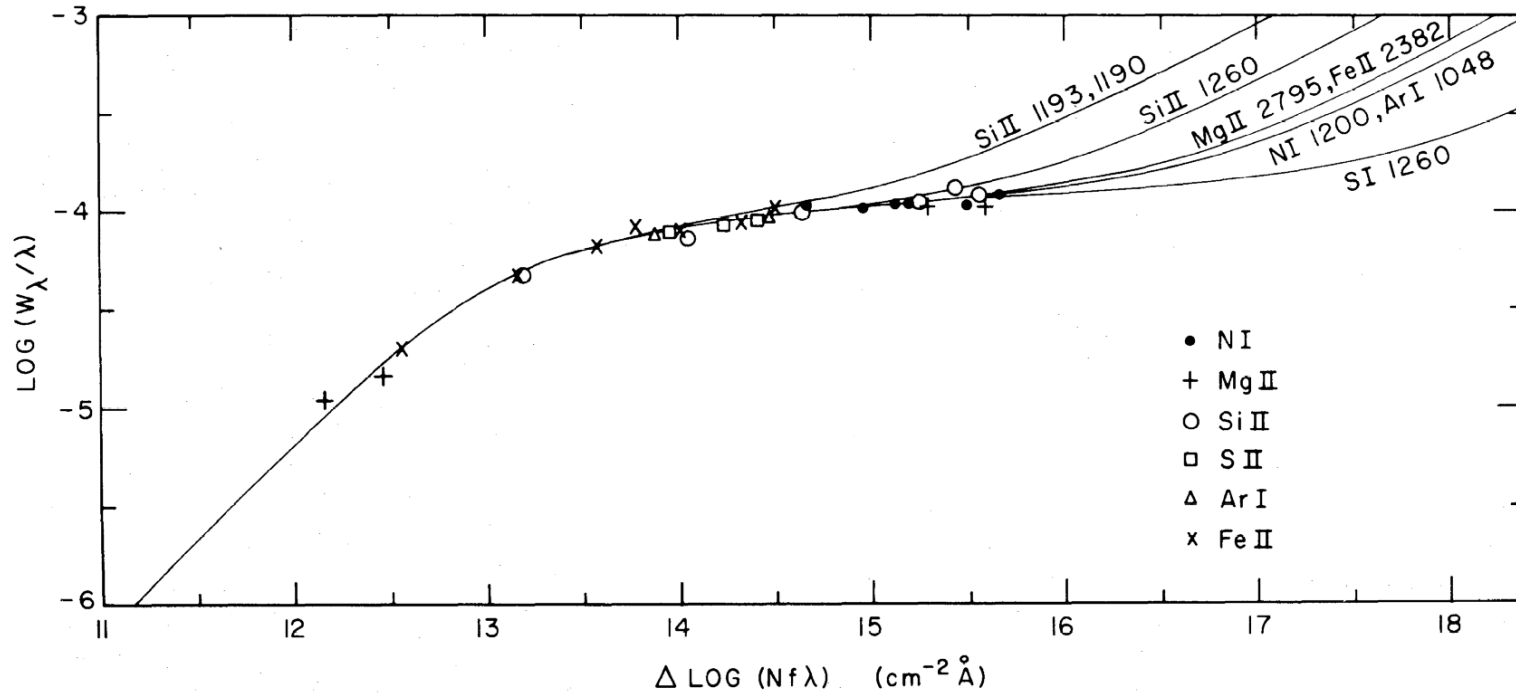


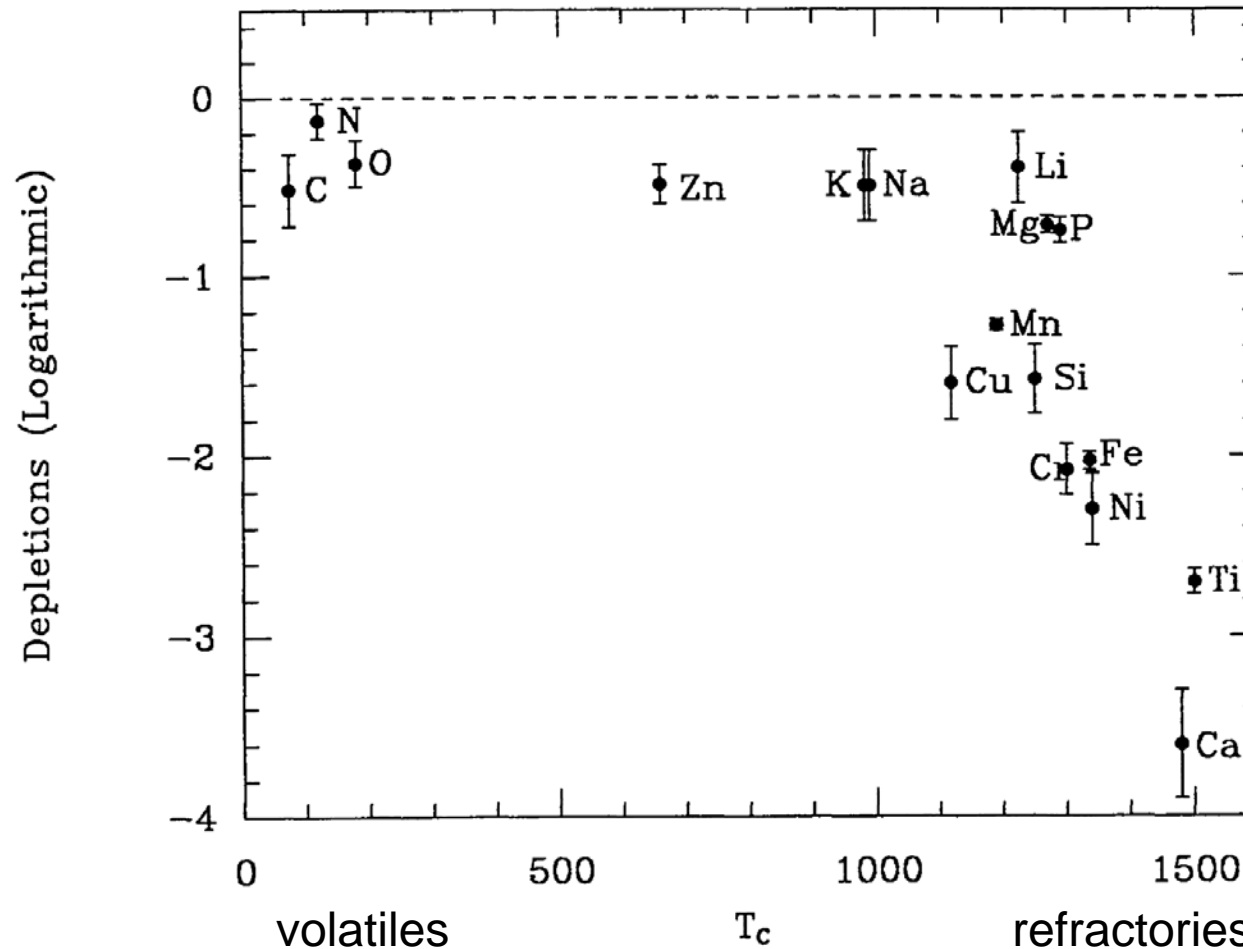
FIG. 5.—Empirical curve of growth for the dominant ion states expected in H I clouds. The solid lines were drawn for a Maxwellian velocity distribution with $b = 6.5 \text{ km s}^{-1}$ and the damping constants appropriate for the lines labeled in the upper right corner. The horizontal scale was labeled to give $\log N(\text{cm}^{-2})$ for Fe II $\lambda 2382$.

Curves are empirical curves of growth for several UV lines, but with the same Doppler parameter.

Results of Abundance Measurements

- Absorption line studies yield gas phase abundances of the astrophysically important elements that determine the physical & chemical properties of the ISM, including the D/H ratio important for cosmology.
- Refractory elements are “depleted” relative to solar; the depletion factor $D(X)$ of species X is
$$D(X) = \text{measured } x(X) / \text{solar } x(X)$$
e.g., $\log D(\text{Ca}) = -4 \Rightarrow$ 10,000 times less Ca in interstellar clouds the solar photosphere. The following plot of depletion vs. condensation temperature suggests that the “missing” elements are in interstellar dust.
- For more results, see recent review, “Diffuse Atomic and Molecular Clouds” Snow & McCall, ARAA 44 367 2006

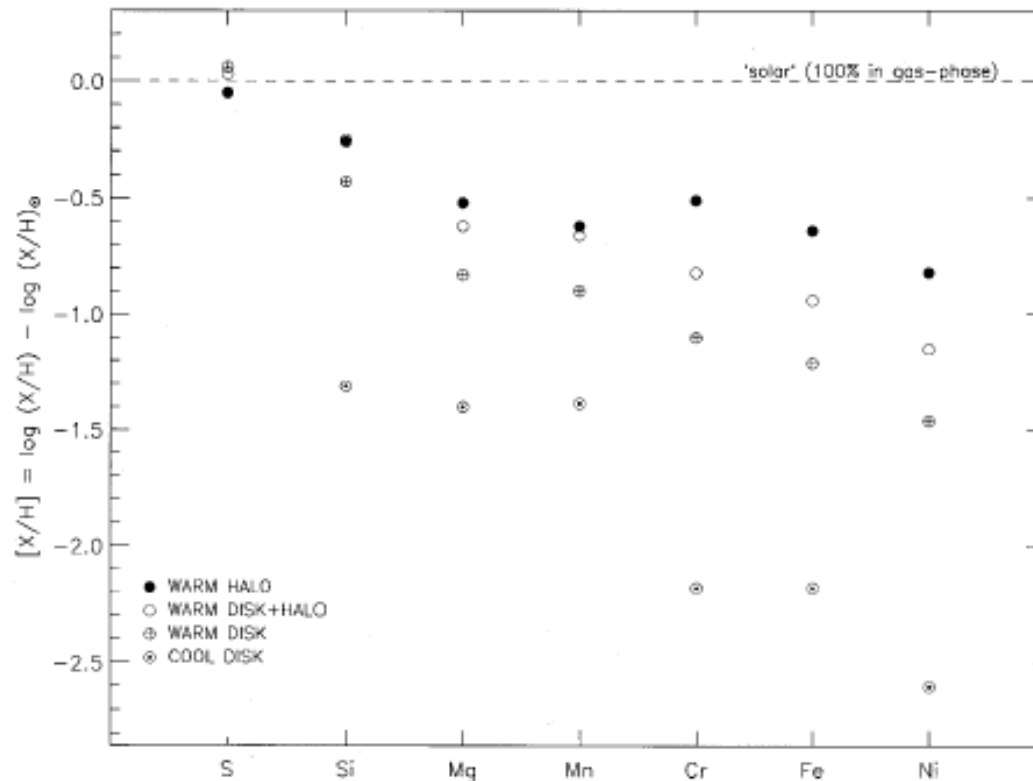
Depletions vs. Condensation Temperature



For more details, see Sembach & Savage, ARAA 34, 279, 1996,
“Interstellar Abundances from Absorption-Line Observations with HST”

Variations in Depletion in the ISM

310 SAVAGE & SEMBACH



warm halo
warm disk + halo
warm disk

cool disk

Figure 6 Gas-phase abundances, $[X/H] = \log(X/H) - \log(X/H)_{\odot}$, of 7 abundant elements for diffuse cloud sight lines in the Galactic disk and halo. The values of $[X/H]$ for halo clouds have been derived from measures of $[X/Zn]$ and the assumption that $[X/Zn] \sim [X/H]$. The data used to construct this figure are in Table 6. The cool disk data points are averages for the cool diffuse clouds toward ξ Per and ζ Oph (Table 5). Note the clear differences in the abundance patterns of the disk and halo gases. The upper envelope of abundances established by the halo cloud values indicates that the halo clouds contain a substantial amount of dust with core material that is difficult to destroy through the processes that inject gas and dust into the halo.